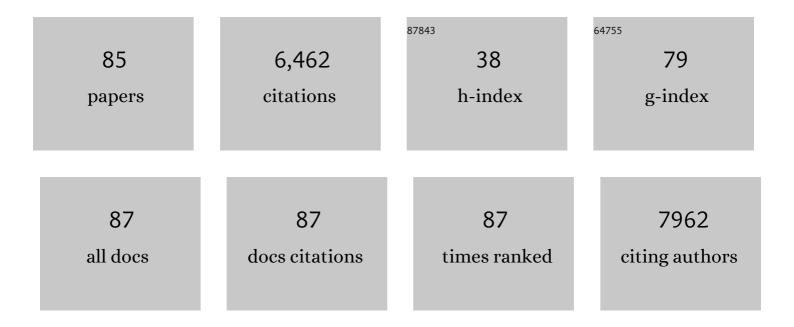
## Umesh V Waghmare

List of Publications by Year in descending order

Source: https://exaly.com/author-pdf/6882684/publications.pdf

Version: 2024-02-01



#	Article	IF	CITATIONS
1	CO2 Utilization Through its Reduction to Methanol: Design of Catalysts Using Quantum Mechanics and Machine Learning. , 2022, 7, 1-11.		3
2	Activation of CO <sub>2</sub> and CH <sub>4</sub> on MgO surfaces: mechanistic insights from first-principles theory. Physical Chemistry Chemical Physics, 2022, 24, 1415-1423.	1.3	4
3	Local Symmetry Breaking Suppresses Thermal Conductivity in Crystalline Solids. Angewandte Chemie, 2022, 134, .	1.6	4
4	Local Symmetry Breaking Suppresses Thermal Conductivity in Crystalline Solids. Angewandte Chemie - International Edition, 2022, 61, .	7.2	16
5	Opportunities and challenges for 2D heterostructures in battery applications: a computational perspective. Nanotechnology, 2022, , .	1.3	1
6	Berry curvature dipole senses topological transition in a moiré superlattice. Nature Physics, 2022, 18, 765-770.	6.5	51
7	Unusual CO <sub>2</sub> Adsorption in ZIF-7: Insight from Raman Spectroscopy and Computational Studies. Inorganic Chemistry, 2022, 61, 11571-11580.	1.9	4
8	Predicting the DNA Conductance Using a Deep Feedforward Neural Network Model. Journal of Chemical Information and Modeling, 2021, 61, 106-114.	2.5	13
9	Modulation of the electronic structure and thermoelectric properties of orthorhombic and cubic SnSe by AgBiSe <sub>2</sub> alloying. Chemical Science, 2021, 12, 13074-13082.	3.7	20
10	<i>Operando</i> Generated Ordered Heterogeneous Catalyst for the Selective Conversion of CO <sub>2</sub> to Methanol. ACS Energy Letters, 2021, 6, 509-516.	8.8	41
11	Enhanced atomic ordering leads to high thermoelectric performance in AgSbTe <sub>2</sub> . Science, 2021, 371, 722-727.	6.0	306
12	Metavalent Bonding in GeSe Leads to High Thermoelectric Performance. Angewandte Chemie - International Edition, 2021, 60, 10350-10358.	7.2	58
13	Metavalent Bonding in GeSe Leads to High Thermoelectric Performance. Angewandte Chemie, 2021, 133, 10438-10446.	1.6	12
14	Magneto-Optical Stark Effect in Fe-Doped CdS Nanocrystals. Nano Letters, 2021, 21, 3798-3804.	4.5	6
15	Flat Phonon Band-Based Mechanism of Amorphization of MOF-5 at Ultra-low Pressures. Journal of Physical Chemistry C, 2021, 125, 14924-14931.	1.5	4
16	Mechanistic insights into the promotional effect of Ni substitution in non-noble metal carbides for highly enhanced water splitting. Applied Catalysis B: Environmental, 2021, 298, 120560.	10.8	41
17	Emphanisis in Cubic (SnSe) <sub>0.5</sub> (AgSbSe <sub>2</sub> ) <sub>0.5</sub> : Dynamical Off-Centering of Anion Leads to Low Thermal Conductivity and High Thermoelectric Performance. Journal of the American Chemical Society, 2021, 143, 16839-16848.	6.6	37
18	Intrinsically Ultralow Thermal Conductivity in Ruddlesden–Popper 2D Perovskite Cs <sub>2</sub> Pbl <sub>2</sub> Cl <sub>2</sub> : Localized Anharmonic Vibrations and Dynamic Octahedral Distortions. Journal of the American Chemical Society, 2020, 142, 15595-15603.	6.6	82

#	Article	IF	CITATIONS
19	Ferroelectric Instability Induced Ultralow Thermal Conductivity and High Thermoelectric Performance in Rhombohedral <i>p</i> -Type GeSe Crystal. Journal of the American Chemical Society, 2020, 142, 12237-12244.	6.6	69
20	Chemical Route to Twisted Graphene, Graphene Oxide and Boron Nitride. Chemistry - A European Journal, 2020, 26, 6499-6503.	1.7	4
21	Scale-free ferroelectricity induced by flat phonon bands in HfO <sub>2</sub> . Science, 2020, 369, 1343-1347.	6.0	231
22	First-principles phonon-based model and theory of martensitic phase transformation in NiTi shape memory alloy. Materialia, 2020, 9, 100602.	1.3	10
23	Intrinsically Low Thermal Conductivity and High Carrier Mobility in Dual Topological Quantum Material, nâ€Type BiTe. Angewandte Chemie, 2020, 132, 4852-4859.	1.6	19
24	Intrinsically Low Thermal Conductivity and High Carrier Mobility in Dual Topological Quantum Material, nâ€Type BiTe. Angewandte Chemie - International Edition, 2020, 59, 4822-4829.	7.2	45
25	Effect of Mn <sup>2+</sup> substitution on the structure, properties and HER activity of cadmium phosphochlorides. RSC Advances, 2020, 10, 5134-5145.	1.7	4
26	Stress-Induced Electronic Structure Modulation of Manganese-Incorporated Ni <sub>2</sub> P Leading to Enhanced Activity for Water Splitting. ACS Applied Energy Materials, 2020, 3, 1271-1278.	2.5	24
27	Destabilizing excitonic insulator phase by pressure tuning of exciton-phonon coupling. Physical Review Research, 2020, 2, .	1.3	9
28	YRuO3 : A quantum weak ferromagnet. Physical Review Materials, 2020, 4, .	0.9	4
29	Theory and Simulations of Lattice Thermal Conduction. , 2019, , 43-67.		0
30	Realization of High Thermoelectric FigureÂof Merit in GeTe by Complementary Co-doping of Bi and In. Joule, 2019, 3, 2565-2580.	11.7	175
31	Synergetic Effect of Ni-Substituted Pd <sub>2</sub> Ge Ordered Intermetallic Nanocomposites for Efficient Electrooxidation of Ethanol in Alkaline Media. ACS Applied Energy Materials, 2019, 2, 7132-7141.	2.5	22
32	Engineering ferroelectric instability to achieve ultralow thermal conductivity and high thermoelectric performance in Sn <sub>1â^'x</sub> Ge <sub>x</sub> Te. Energy and Environmental Science, 2019, 12, 589-595.	15.6	155
33	Structural Features and HER activity of Cadmium Phosphohalides. Angewandte Chemie - International Edition, 2019, 58, 6926-6931.	7.2	8
34	Microscopic Origin of Piezoelectricity in Lead-Free Halide Perovskite: Application in Nanogenerator Design. ACS Energy Letters, 2019, 4, 1004-1011.	8.8	65
35	Bonding heterogeneity and lone pair induced anharmonicity resulted in ultralow thermal conductivity and promising thermoelectric properties in n-type AgPbBiSe <sub>3</sub> . Chemical Science, 2019, 10, 4905-4913.	3.7	74
36	Structural Features and HER activity of Cadmium Phosphohalides. Angewandte Chemie, 2019, 131, 7000-7005.	1.6	2

#	Article	IF	CITATIONS
37	Transient Species Mediating Energy Transfer to Spin-Forbidden Mn d States in Il–VI Semiconductor Quantum Dots. ACS Energy Letters, 2019, 4, 729-735.	8.8	26
38	Van der Waals hetero-structures of 1H-MoS <sub>2</sub> and N-substituted graphene for catalysis of hydrogen evolution reaction. Materials Research Express, 2019, 6, 124006.	0.8	4
39	Realization of Both n- and p-Type GeTe Thermoelectrics: Electronic Structure Modulation by AgBiSe <sub>2</sub> Alloying. Journal of the American Chemical Society, 2019, 141, 19505-19512.	6.6	69
40	Ultralow Thermal Conductivity in Chain-like TISe Due to Inherent Tl <sup>+</sup> Rattling. Journal of the American Chemical Society, 2019, 141, 20293-20299.	6.6	61
41	Machine Learning Constrained with Dimensional Analysis and Scaling Laws: Simple, Transferable, and Interpretable Models of Materials from Small Datasets. Chemistry of Materials, 2019, 31, 314-321.	3.2	23
42	Soft Phonon Modes Leading to Ultralow Thermal Conductivity and High Thermoelectric Performance in AgCuTe. Angewandte Chemie - International Edition, 2018, 57, 4043-4047.	7.2	70
43	Soft Phonon Modes Leading to Ultralow Thermal Conductivity and High Thermoelectric Performance in AgCuTe. Angewandte Chemie, 2018, 130, 4107-4111.	1.6	21
44	Origin of the monolayer Raman signature in hexagonal boron nitride: a first-principles analysis. Journal of Physics Condensed Matter, 2018, 30, 185701.	0.7	3
45	Localized Vibrations of Bi Bilayer Leading to Ultralow Lattice Thermal Conductivity and High Thermoelectric Performance in Weak Topological Insulator <i>n-</i> Type BiSe. Journal of the American Chemical Society, 2018, 140, 5866-5872.	6.6	137
46	Unique Features of the Photocatalytic Reduction of H <sub>2</sub> O and CO <sub>2</sub> by New Catalysts Based on the Analogues of CdS, Cd <sub>4</sub> P <sub>2</sub> X <sub>3</sub> (X = Cl, Br, I). ACS Applied Materials & Interfaces, 2018, 10, 2526-2536.	4.0	20
47	TiNF and Related Analogues of TiO <sub>2</sub> : A Combined Experimental and Theoretical Study. ChemPhysChem, 2018, 19, 3410-3417.	1.0	7
48	Stabilizing nâ€Type Cubic GeSe by Entropyâ€Driven Alloying of AgBiSe <sub>2</sub> : Ultralow Thermal Conductivity and Promising Thermoelectric Performance. Angewandte Chemie - International Edition, 2018, 57, 15167-15171.	7.2	66
49	Stabilizing nâ€Type Cubic GeSe by Entropyâ€Driven Alloying of AgBiSe <sub>2</sub> : Ultralow Thermal Conductivity and Promising Thermoelectric Performance. Angewandte Chemie, 2018, 130, 15387-15391.	1.6	21
50	Experimental and first-principles studies of BiVO4/BiV1-xMnxO4-y n-n+ homojunction for efficient charge carrier separation in sunlight induced water splitting. International Journal of Hydrogen Energy, 2018, 43, 15815-15822.	3.8	8
51	Electronic structure and properties of Cd 4 As 2 Br 3 and Cd 4 Sb 2 I 3 , analogues of CdSe and CdTe. Solid State Communications, 2017, 255-256, 5-10.	0.9	2
52	Intrinsic Rattler-Induced Low Thermal Conductivity in Zintl Type TlInTe <sub>2</sub> . Journal of the American Chemical Society, 2017, 139, 4350-4353.	6.6	177
53	Machine Learning and Statistical Analysis for Materials Science: Stability and Transferability of Fingerprint Descriptors and Chemical Insights. Chemistry of Materials, 2017, 29, 4190-4201.	3.2	64
54	Emergence of a weak topological insulator from the Bi <i>x</i> Se <i>y</i> family. Applied Physics Letters, 2017, 110, .	1.5	38

#	Article	IF	CITATIONS
55	Is There a Lower Size Limit for Superconductivity?. Nano Letters, 2017, 17, 7027-7032.	4.5	8
56	Photochemical Water Splitting by Bismuth Chalcogenide Topological Insulators. ChemPhysChem, 2017, 18, 2322-2327.	1.0	54
57	Low Thermal Conductivity and High Thermoelectric Performance in Sb and Bi Codoped GeTe: Complementary Effect of Band Convergence and Nanostructuring. Chemistry of Materials, 2017, 29, 10426-10435.	3.2	117
58	The Origin of Ultralow Thermal Conductivity in InTe: Loneâ€Pairâ€Induced Anharmonic Rattling. Angewandte Chemie - International Edition, 2016, 55, 7792-7796.	7.2	145
59	Structural, Optical, and Electronic Properties of Wide Bandgap Perovskites: Experimental and Theoretical Investigations. Journal of Physical Chemistry A, 2016, 120, 3917-3923.	1.1	66
60	Local ferroelectricity in thermoelectric SnTe above room temperature driven by competing phonon instabilities and soft resonant bonding. Journal of Materiomics, 2016, 2, 196-202.	2.8	26
61	High Power Factor and Enhanced Thermoelectric Performance of SnTe-AgInTe <sub>2</sub> : Synergistic Effect of Resonance Level and Valence Band Convergence. Journal of the American Chemical Society, 2016, 138, 13068-13075.	6.6	214
62	Accurate first-principles structures and energies of diversely bonded systems from an efficient density functional. Nature Chemistry, 2016, 8, 831-836.	6.6	698
63	Structure and Properties of Cd <sub>4</sub> P <sub>2</sub> Cl <sub>3</sub> , an Analogue of CdS. Journal of Physical Chemistry C, 2016, 120, 15063-15069.	1.5	13
64	Thermoelectric properties of materials with nontrivial electronic topology. Journal of Materials Chemistry C, 2015, 3, 12130-12139.	2.7	69
65	Mg Alloying in SnTe Facilitates Valence Band Convergence and Optimizes Thermoelectric Properties. Chemistry of Materials, 2015, 27, 581-587.	3.2	390
66	Engineering the electronic bandgaps and band edge positions in carbon-substituted 2D boron nitride: a first-principles investigation. Physical Chemistry Chemical Physics, 2015, 17, 13547-13552.	1.3	35
67	Ordered Pd <sub>2</sub> Ge Intermetallic Nanoparticles as Highly Efficient and Robust Catalyst for Ethanol Oxidation. Chemistry of Materials, 2015, 27, 7459-7467.	3.2	61
68	First-Principles Theory, Coarse-Grained Models, and Simulations of Ferroelectrics. Accounts of Chemical Research, 2014, 47, 3242-3249.	7.6	10
69	Borocarbonitrides, BxCyNz. Journal of Materials Chemistry A, 2013, 1, 5806.	5.2	143
70	Intrinsic buckling strength of graphene: First-principles density functional theory calculations. Physical Review B, 2010, 82, .	1.1	30
71	Synthesis, Structure, and Properties of Boron―and Nitrogenâ€Doped Graphene. Advanced Materials, 2009, 21, 4726-4730.	11.1	569
72	Enhanced dielectric response of ZrO2 upon Ti doping and introduction of O vacancies. Journal of Applied Physics, 2008, 103, .	1.1	9

#	Article	IF	CITATIONS
73	Hydrogen Spillover on <i>CeO</i> <sub>2</sub> / <i>Pt</i> : Enhanced Storage of Active Hydrogen. Chemistry of Materials, 2007, 19, 6430-6436.	3.2	97
74	Origin of Enhanced Reducibility/Oxygen Storage Capacity of Ce1-xTixO2Compared to CeO2or TiO2. Chemistry of Materials, 2006, 18, 3249-3256.	3.2	173
75	InMnO3: A biferroic. Journal of Applied Physics, 2006, 100, 076104.	1.1	28
76	BiferroicYCrO3. Physical Review B, 2005, 72, .	1.1	209
77	First-principles indicators of metallicity and cation off-centricity in the IV-VI rocksalt chalcogenides of divalent Ge, Sn, and Pb. Physical Review B, 2003, 67, .	1.1	299
78	Ab initio statistical mechanics of the ferroelectric phase transition inPbTiO3. Physical Review B, 1997, 55, 6161-6173.	1.1	308
79	Lattice instabilities, anharmonicity and phase transitions in PbZrO3from first principles. Ferroelectrics, 1997, 194, 135-147.	0.3	39
80	Strain coupling in perovskite structural transitions: A first principles approach. Ferroelectrics, 1997, 194, 119-134.	0.3	11
81	Lattice Instabilities, Anharmonicity and Phase Transitions in PbTiO3 and PbZrO3. Materials Research Society Symposia Proceedings, 1995, 408, 305.	0.1	0
82	Localized basis for effective lattice Hamiltonians: Lattice Wannier functions. Physical Review B, 1995, 52, 13236-13246.	1.1	93
83	Ferroelectric phase transitions: A first-principles approach. Ferroelectrics, 1995, 164, 15-32.	0.3	35
84	First-principles model hamiltonians for ferroelectric phase transitions. Ferroelectrics, 1994, 151, 59-68.	0.3	9
85	First-principles model hamiltonians for ferroelectric phase transitions. Ferroelectrics, 1992, 136, 147-156.	0.3	24